Ray Density Analysis for Virtual Spectrophotometers

GLADIMIR V. G. BARANOSKI JON G. ROKNE GUANGWU XU

Department of Computer Science, The University of Calgary, 2500 University Dr. N.W., Calgary, Alberta, T2N 1N4, Canada

Tecnical Report 99/639/02

Abstract

Virtual spectrophotometric measurements have important applications in physically-based rendering. These measurements can be used to evaluate reflectance and transmittance models through comparisons with actual spectrophotometric measurements. Moreover, they can also be used to generate spectrophotometric data, which are dependent either on the wavelength or on the illuminating geometry of the incident radiation, from previously validated models. In this paper the ray casting based formulation for virtual spectrophotometers is discussed and a mathematical bound, based on probability theory, is proposed to determine the number of rays needed to obtain asymptotically convergent readings. Specifically, the exponential Chebyshev inequality is introduced to determine the ray density required to obtain reflectance and transmittance measurements with a high reliability/cost ratio. Practical experiments are provided to illustrate the validity and usefulness of the proposed approach.

1. Introduction

The group of measurements necessary to characterize both the color and surface finish of an object is called the *measurement of appearance* of an object [15]. This group of measurements involves the spectral energy distribution of propagated light, measured in terms of reflectance and transmittance, and the spatial distribution of that light, measured in terms of the bidirectional reflectance distribution function (BRDF) and the bidirectional transmittance distribution function (BTDF). The variations in the spectral energy distribution affect appearance characteristics such as hue, lightness and saturation, while the changes in the spatial distribution affect appearance characteristics such as gloss, reflection haze, transmission haze, luster and translucency [15].

A spectrophotometer is defined as an instrument for measuring spectral distribution of reflected or transmitted radiant power, and spectrophotometry is defined as the quantitative measurement of reflection or transmission properties as a function of wavelength [8]. Spectrophotometers can also be used to determine the absorption characteristics of an object as a function of wavelength. They are important basic tools for fundamental research in colorimetry [19], solar engineering [9] and remote sensing [14]. In this paper we are interested in computer simulations of these devices, henceforth called virtual spectrophotometers, aimed at physically-based rendering applications. As pointed out by Lalonde and Fournier [17], the use of virtual measurement devices gives us control over the spectral data generation and allows us to perform experiments at different sampling resolutions, which are essential requirements for these applications.

Among the main applications of virtual spectrophotometers, two are especially relevant for physically-based rendering. The first application corresponds to virtual spectrophotometric measurements aimed at the testing and validation of reflectance models through comparisons with actual spectrophotometric measurements. In this case, the formulation of a virtual spectrophotometer has to reproduce actual measurement conditions as faithfully as possible. The second application corresponds to spectrophotometric data generation from previously validated models, which may involve a large number of measurements regarding different wavelengths and illuminating geometries. Although these applications usually involve reflectance and transmittance measurements, they can be extended to other phenomena as well. For example, commercial surfaces such as paint, plastics, papers and textiles, both matte and glossy, show some degree of retroreflection, *i.e.*, reflectance in the incident direction. This phenomenon can be measured easily using a virtual spectrophotometer when an appropriate reflectance model for such a surface is provided.

Virtual spectrophotometers are normally implemented using ray casting algorithms combined with standard Monte Carlo methods [12] applied to particle transport simulations [4, 5]. The purpose of these devices is to determine the numerical value of an estimand, or expected value, to which the readings of reflectance, or transmittance, of a model converge. This estimand will correspond to a reflectance, or transmittance, value for a given wavelength and illuminating geometry. When discussing the virtual spectrophotometric measurements in this paper it shall be noted that we will focus on the reflectance, implicitly including the transmittance by analogy, since it is handled similarly to reflectance.

Due to their stochastic nature the virtual spectrophotometers may sometimes provide estimates with low variance with respect to the estimand in the early stages of the simulation, *i.e.*, after using a small number of sample rays. Since the value of the estimand is unknown before the simulation, these earlier estimates are not reliable, and estimates within the region of asymptotic convergence of the estimand are, therefore, desired. In fact, if one knew *a priori* the value of the estimand there would be no point in carrying out virtual spectrophotometric measurements. To ensure that the estimates for a given model are within the asymptotic convergence region, a brute-force approach, which consists of using a very large number of sample rays (in some cases up to 10^8 rays [7]), is usually applied. However, the application of this strategy results in a high computational overhead in terms of processing time. This overhead becomes rather prohibitive when the simulations involve a large number of measurements for different wavelengths and finer incidence sampling resolutions.

In this paper we perform a ray density analysis to determine the least number of rays required to obtain estimates within the region of asymptotic convergence of the estimand with high confidence, and, consequently, substantially reduce the processing time. For the reason mentioned earlier, the determination of an appropriate ray density, or sample size, shall not depend on the knowledge about the value of the estimand or on its variance. In order to fulfill this guideline we present a mathematical criterion derived from a probability concept, namely the *exponential* Chebyshev inequality [24], and adapt it to the requirements of spectrophotometric measurements aimed at rendering applications. Numerical experiments involving reflectance models with different levels of complexity are shown to illustrate its applicability.

The remainder of this paper is organized as follows. The next section describes the general characteristics of actual spectrophotometers and the stochastic formulation of virtual spectrophotometers. Section 3 discusses the applicability of inequalities usually used in particle transport simulations and introduces the *exponential* Chebyshev inequality to the rendering literature. Section 4 describes the experimental procedures used in the evaluation of the usefulness of the proposed approach. Section 5 discusses the results of the experiments and performance issues. Finally, the paper closes with a summary and directions for future research.

2. Virtual Spectrophotometry

Before presenting the formulation of virtual spectrophotometers, we shall briefly review some relevant terms and definitions and describe the general characteristics of real spectrophotometers.

2.1. Reflectance and Transmittance Terms

As mentioned in the previous section, reflectance and transmittance are important terms used in the description of the appearance of objects or surfaces. The reflectance of a given surface can be defined as the fraction of light at wavelength λ incident from a direction ψ_i that is neither absorbed into nor transmitted through the surface [22], and it is denoted by $\rho(\lambda, \psi_i)$. Similarly, the fraction of light transmitted through the surface is called the transmittance, $\tau(\lambda, \psi_i)$. The light that is neither reflected nor transmitted by the surface is absorbed. The parameter that describes the amount of absorbed light is absorptance [1], denoted by $\alpha(\lambda, \psi_i)$. The sum of the reflectance, transmittance and absorptance is one.

In computer graphics we are interested in the amount of light hitting a surface or film plane during a set period of time. Radiant power or flux, denoted by Φ (measured in Watts, W, or $\frac{J}{s}$), is, therefore, often used as pointed out by Shirley [22]. In this context reflectance can be defined as the ratio of reflected flux to incident flux [20]. Similarly, transmittance can be defined as the ratio of transmitted flux to incident flux.

Other important terms used in the description of appearance of objects are the reflectance and transmittance factors. The reflectance factor, denoted by R, is defined as the ratio of flux reflected from the specimen to flux reflected from the perfect reflecting diffuser under the same spectral and geometrical conditions of measurement [8]. Similarly, the transmittance factor, denoted by T, is defined as the ratio of flux transmitted by the specimen to flux transmitted by the perfect transmitting diffuser under the same spectral and geometrical conditions of measurement.

There are different types of reflectance (or transmittance) depending on the incident and reflected (transmitted) solid angles associated with the incident and reflected (transmitted) beam geometry. Nicodemus *et al.* [20] distinguishes three types of solid angles: directional, conical and hemispherical. There are, therefore, nine possible combinations of solid angles resulting in nine types of reflectance. For instance, if the incident beam is collimated and the collection of the reflected flux is performed taking into account the whole hemisphere above the plane of the specimen, then directional-hemispherical reflectance is being measured.

2.2. General Characteristics of Actual Spectrophotometers

Actual measurements of reflectance and transmittance are performed using spectrophotometers equipped with an integrating sphere. An integrating sphere is usually used to measure the hemispherical reflectance factor, *i.e.* a reflectance factor regarding a hemispherical reflected solid angle [20]. The numerical values of the reflectance and the transmittance factor are, however, identical under the conditions of hemispherical collection [10].

For absolute measurements, the sphere wall is the standard, and the integrating sphere theory [11] compensates for the absolute reflectance of the sphere wall by mathematically treating the wall reflectance as unity. Hence, as pointed out by Zerlaut and Anderson [26], the hemispherical measurements made with such integrating spheres correspond to absolute values of reflectance (or transmittance), which are subject to small errors associated with factors such as aperture losses, small values of non-uniformity of sphere wall reflectance and stray reflectance from sample mounts.

The accuracy of a real spectrophotometer is estimated by the ability of the instrument to replicate a measurement for a given specimen under same spectral and geometrical conditions [16]. The best-designed, best-constructed, and best-calibrated spectrophotometers still yield results that differ from one measurement to the next [19]. According to MacAdam [19], the differences among readings should be quite small and randomly different. These differences, or uncertainties, are net results of combinations of many small fluctuations due to mutually unrelated variations of different components of the instrument, different factors in the environment and how the specimen is handled. In theory, a spectrophotometer is considered to be of high accuracy if the spectral measurements have an uncertainty, μ, of approximately ± 0.001 [16, 19]. This means that at one time the device may read, for instance, a reflectance value equal to 0.375, but at other times it may read values as low as 0.374 or as high as 0.376. In practice, however, spectrophotometers usually have an absolute accuracy between 0.993 and 0.995, *i.e.*, an uncertainty between ± 0.007 and ± 0.005 measurement units [26].

2.3. Formulation of Virtual Spectrophotometers

In the following presentation, light propagation is described in terms of ray or geometrical optics, where light is assumed to be composed of non-interacting straight rays, each of them carrying a certain amount of energy [18]. Emitters and specimens used in actual measurements usually have circular areas [7, 11, 14, 26], which can be represented by disks with radii r_1 and r_2 separated by a distance D (Fig. 1). Using geometrical optics, a spectrophotometer with integrating sphere is simulated by sending (or shooting) sample rays from the emitter towards the specimen. These rays arrive at the specimen through a solid angle, $\vec{\omega}_i$, in the direction of incidence ψ_i, which is given by a pair of spherical coordinates (ϕ_i, θ_i) (Fig. 1). We denote the total number of sample rays used in a virtual spectrophotometric measurement by N. For the sake of compactness we may also represent the sample ray density by $\log N$ (base 10).

Consider a total number of N rays shot towards the specimen for a given wavelength λ. One can assume that each ray carries the same amount of radiant power, Φ. If the total radiant power to be shot is Φ_i, then, as stated by Shirley [22], the radiant power carried by each ray is given by:

$$\Phi_{ray}(\lambda) = \frac{\Phi_i(\lambda)}{N} \tag{1}$$

Recall that reflectance describes the ratio of reflected power to incident radiant power and transmittance describes the ratio of transmitted radiant power to incident power [20]. Considering this ratio, if m rays are reflected towards the upper hemisphere Ω_r, the reflectance of the specimen with respect to a given wavelength λ of the incident light will be given by:

$$\rho(\lambda, \vec{\omega}_i, \Omega_r) = \frac{m}{N} \tag{2}$$

Therefore, since one can simply count the number of rays reflected to the upper hemisphere to determine a specimen's reflectance, a virtual spectrophotometer does not need to use an integrating sphere to collect the reflected rays. The specimen's transmittance is calculated in a similar manner, *i.e.*, by counting the number of rays transmitted to the lower hemisphere.

For applications involving data generation from a previously validated model, the sample rays are collimated since we are

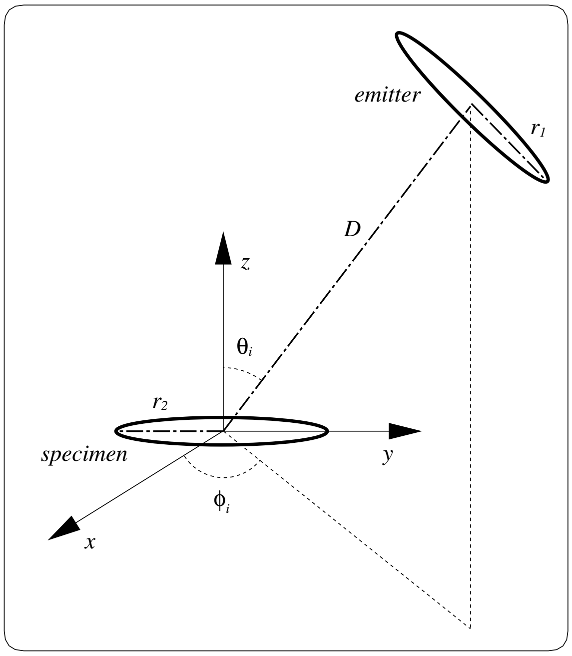

Fig. 1: *Sketch of a virtual spectrophotometer.*

basically measuring directional-hemispherical reflectance [20]. In this case, the sample rays have the same origin and hit the specimen at the same point. For applications involving comparisons with actual measurements, as mentioned earlier, the actual measurement conditions must be reproduced as faithfully as possible. In these situations we are measuring conical-hemispherical reflectance [20], which requires the generation of sample rays distributed angularly according to the geometrical arrangement of the surfaces used to represent the emitter and the specimen.

As mentioned by Crowther [7], the incident radiation from an emitter shows no preference for one angular region over the other. So, in order to simulate these measurement conditions, the origins and targets of the rays are random points (or sample points) chosen on the disks used to represent the emitter and the specimen respectively.

Several sampling strategies may be used to select the sample points on the disks [22]. We applied two different strategies to select the random points used in the first set of experiments shown in Sec. 5. In these experiments we investigated the applicability of the proposed bound for ray density (Sec. 3.2). The use of different sampling strategies as well as different reflectance models in these experiments allowed us to increase our scope of observations.

One of the sampling strategies used in our experiments is based on standard random sampling [22]. It consists of generating sample points inside a square with sides $2r$ and throwing away points lying outside an inscribed disk of radius r [7]. The sample points in the square are generated using uniformly distributed random numbers ξ_1 and ξ_2 on the interval $[0,1]$ and the following transformation:

$$(x,y) = (2r\xi_1 - r, 2r\xi_2 - r) \tag{3}$$

where the pair (x,y) corresponds to the coordinates of a sample point.

The other strategy used in our experiments is based on the classical Monte Carlo stratified sampling [12] or jittered sampling [22]. It uses a warping transformation to guarantee that the sample points are reasonably equidistributed on a disk. This transformation is based on the following probability distribution function [12] (PDF) [23]:

$$\Gamma(x,y) = \frac{1}{\pi r^2} \tag{4}$$

which enables the computation of the pair (x,y) through the following warping function:

$$(x,y) = (2\pi\xi_1, r\sqrt{\xi_2}) \tag{5}$$

In terms of accuracy, it can be seen from the experiments shown in Sec. 5 (Fig. 2) that both strategies lead to a similar asymptotic convergence of the estimates. In terms of execution time, an appreciable difference (over 85%) between the two strategies is noted when we perform a stand-alone generation of a reasonably large number of sample points (Table 1). This difference can be attributed to the relatively long time required to compute the trigonometric functions used by the jittering-based strategy. The effect of this difference on the overall performance of a virtual spectrophotometer tend, however, to become less noticeable as we perform measurements for more complex reflectance models (Figs. 3 and 4).

strategy	$\log N$		
	6	7	8
random	$2s$	$18s$	$178s$
jittering	$4s$	$34s$	$340s$

Table 1: *Comparison of execution times (given in seconds) of the stand-alone generation of N sample points using a standard random-based strategy and a jittering-based strategy. These time measurements were performed on a SGI R5000.*

After generating the coordinates x and y of a sample point, using either approach mentioned above, the z coordinate is added. For a sample point on the specimen, z is equal to zero, and, for a sample point on the emitter, z will correspond to the distance D between the disks (Fig. 1), which is given by the radius of the integrating sphere of a real spectrophotometer. Finally, to obtain the origin of a sample ray, the corresponding sample point (x, y, z) on the emitter shall be rotated according to a specified incidence geometry given by ϕ_i and θ_i (Fig. 1).

3. Ray Density Analysis

The main question to be addressed when performing a virtual spectrophotometric measurement is how many rays should be cast by the emitter element, that is, how large should N be. According to the Bernoulli theorem (Sec. 3.1), using a sufficiently large number of sample rays, one will have a high probability to obtain estimates within the region of asymptotic convergence of the expected value of reflectance, or transmittance, being measured. However, as shown by numerical experiments presented in Sec. 5 (Fig. 3), the processing time grows rapidly with respect to the total number of sample rays N.

The purpose of the following analysis is to determine a satisfactory bound for N such that we can obtain estimates of reflectance ρ, or transmittance τ, with a higher reliability/cost ratio. In other words, we want to obtain estimates within the region of asymptotic convergence and reduce the processing time. In this context the term satisfactory means taking into account the uncertainty of the real spectrophotometer, whose readings we are comparing the virtual spectrophotometric measurements with, and aiming at an error tolerance for ρ, or τ, compatible with rendering requirements. Before getting to the specifics of the criterion proposed in this paper to select a satisfactory bound for N, we review some relevant concepts.

3.1. Bernoulli Theorem and Chebyshev Inequality

A random variable ζ that takes two values 1 and 0 with probabilities p ("success") and q ("failure"), where $p+q=1$, is called a Bernoulli random variable [24]. A probabilistic model of k independent sampling experiments with two possible outcomes occurring with probabilities p and q is called a Bernoulli trial [25].

Suppose that $\zeta_1, \zeta_2, \ldots, \zeta_k$ are independent Bernoulli variables. The expectation of a Bernoulli variable ζ_i is given by:

$$E(\zeta_i) = p \tag{6}$$

As stated by Shiryaev [24], if we define the sum of k Bernoulli random variables as:

$$S_k = \sum_{i=1}^{k} \zeta_i \tag{7}$$

it follows that:

$$E(S_k) = kp \tag{8}$$

As stated by Chiang [6], for sufficiently large k, the relative frequency $\frac{S_k}{k}$ becomes and remains close to p with a probability of one. Jacob Bernoulli, in his posthumous book *Ars Conjectandi* (1713), published a theorem [25] that formally describes this fact. The Bernoulli theorem states that, for every strip of width $\varepsilon > 0$ and error tolerance $\delta > 0$, there is a number K such that, for $k = K+1, K+2, \ldots$,

$$P\left\{\left|\frac{S_k}{k} - p\right| \geq \varepsilon\right\} > 1 - \delta \tag{9}$$

where $P\{w\}$ means the probability of w.

The particle transport simulation using Monte Carlo methods can be seen as a Bernoulli trial [4,5]. In this context, a general result of probability theory, known as the Chebyshev inequality [6,25], can be used to determine the number of samples needed to obtain estimates with a certain error tolerance in a strip of width ε. This inequality states that:

$$P\{\zeta \geq \varepsilon\} \leq \frac{E(\zeta)}{\varepsilon} \qquad \forall \varepsilon > 0 \tag{10}$$

From the Chebyshev inequality it can be shown [24] that:

$$P\left\{\left|\frac{S_k}{k} - p\right| \geq \varepsilon\right\} \leq \frac{pq}{k\varepsilon^2} \leq \frac{1}{4k\varepsilon^2} \tag{11}$$

Recall from probability theory that:

$$P\{|w| < \varepsilon\} = 1 - P\{|w| \geq \varepsilon\} \tag{12}$$

Hence, we can rewrite the inequality given by Eq. 11 as:

$$P\left\{\left|\frac{S_k}{k} - p\right| < \varepsilon\right\} \geq 1 - \frac{1}{4k\varepsilon^2} \tag{13}$$

The error tolerance in an estimation is a given parameter (usually small). Theoretically δ is a positive number such that:

$$\delta \geq 1 - P\left\{\left|\frac{S_k}{k} - p\right| < \varepsilon\right\} \tag{14}$$

Then, to satisfy the above inequality, it is required that:

$$\delta \geq \frac{1}{4k\varepsilon^2} \tag{15}$$

Therefore, from the Chebyshev inequality, the least number of sampling experiments required to obtain estimates with an error tolerance δ is given by:

$$k_c = \left\lceil \frac{1}{4\varepsilon^2\delta} \right\rceil \tag{16}$$

3.2. Applying the Exponential Chebyshev Inequality to Virtual Spectrophotometry

The *exponential* Chebyshev inequality [24] can be used to obtain a more precise a bound for the number of sampling experiments than the bound derived from the ordinary Chebyshev inequality described in the previous section. Assuming $w \geq 0$ and $\nu > 0$, the "exponential form" of the Chebyshev inequality states that:

$$P\{w \geq \varepsilon\} = P\{e^{\nu w} \geq e^{\nu\varepsilon}\} \leq E\{e^{\nu(w-\varepsilon)}\} \tag{17}$$

From the *exponential* Chebyshev inequality it can be shown [24] that:

$$P\left\{\left|\frac{S_k}{k} - p\right| \geq \varepsilon\right\} \leq 2e^{-2k\varepsilon^2} \tag{18}$$

Using Eq. 12 it follows that:

$$P\left\{\left|\frac{S_k}{k} - p\right| < \varepsilon\right\} \geq 1 - 2e^{-2k\varepsilon^2} \tag{19}$$

From a reasoning similar to the one used to obtain the inequality given by Eq. 15, it follows that:

$$\delta \geq 2e^{-2k\varepsilon^2} \tag{20}$$

Hence, from the *exponential* Chebyshev inequality, the least number of sampling experiments need to obtain estimates with an error tolerance δ is given by:

$$k_e = \left\lceil \frac{\ln(\frac{2}{\delta})}{2\varepsilon^2} \right\rceil \tag{21}$$

As mentioned by Shiryaev [24], using the theory of limits, it is possible to compare the bound k_c provided by the ordinary Chebyshev inequality with the bound k_e provided by the *exponential* Chebyshev inequality:

$$\lim_{\delta \to 0} \frac{k_c(\delta)}{k_e(\delta)} = \lim_{\delta \to 0} \frac{1}{2\delta \ln(\frac{2}{\delta})} = \infty \tag{22}$$

It is clear from the previous expression that when $\delta \to 0$, k_e is tighter than k_c. In virtual spectrophotometric measurements oftentimes one needs relatively low accuracy estimates however. For exmaple, as mentioned by Nievergelt [21], illuminating engineers need solutions accurate to only 1% to 10%, since humans do not perceive finer variations of light. This accuracy requirement is also valid for spectrophotometry aimed at rendering applications. Before going further in the analysis of this issue, we shall describe how the probability concepts presented so far fit into virtual spectrophotometry.

We can think of a virtual spectrophotometric reflectance measurement as a Bernoulli trial, and the sample rays as Bernoulli random variables. Viewed in this context, the reflectance ρ, or the probability of a sample ray being reflected to the upper hemisphere, corresponds to p. Also, the total number of sample rays N corresponds to k, and the number of rays m reflected to the upper hemisphere corresponds to S_k. Moreover, the uncertainty μ of the real spectrophotometer, whose readings we intend to compare the virtual spectrophotometric measurements with, can be associated with ε. Therefore, Eqs. 13 and 19, and the respective bounds derived from them, can be rewritten using terms applied to virtual spectrophotometry.

For instance, Eq. 19 can be rewritten as:

$$P\left\{ \left| \frac{m}{N} - \rho \right| < \mu \right\} \geq 1 - 2e^{-2N\mu^2} \tag{23}$$

and the bound on the number of sample rays derived from the *exponential* Chebyshev inequality can be rewritten as:

$$N = \left\lceil \frac{\ln(\frac{2}{\delta})}{2\mu^2} \right\rceil \tag{24}$$

The figures presented in Table 2 show that, even for relatively low accuracy measurements, the bound derived from the *exponential* Chebyshev inequality results in a number of sample rays considerably smaller than the number given by the bound derived from the ordinary Chebyshev inequality. Notice that these figures are given in a logarithmic scale. In Sec. 5 we present experiments that illustrate the applicability of the *exponential* Chebyshev bound in virtual spectrophotometry, and highlight the significant time savings that can be obtained from its application.

δ	ordinary Chebyshev $\log N$	*exponential* Chebyshev $\log N$
0.001	7.0	5.18
0.01	6.0	5.02
0.1	5.0	4.77

Table 2: *Comparison of bounds on the number of sample rays required to obtain estimates with an error tolerance given by* δ *and using* $\mu = 0.005$.

4. Experimental Procedures

We used reflectance models with different levels of complexity to illustrate the applicability of the proposed bound for the ray density (Eq. 24) under different measurement conditions. The first model used in our experiments corresponds to a simplified reflectance model for dielectrics, similar to the one described by Shirley [22]. It essentially consists of computing the Fresnel coefficient (using Fresnel equations [13]) when a ray hits the specimen. This coefficient, denoted by F, is compared with a random number ξ uniformly distributed on the interval $[0,1]$. If $F \leq \xi$, then the sample ray is reflected to the upper hemisphere. This model does not account for wavelength dependency and uses the index of refraction, denoted by η, of the dielectric as parameter. For the experiments with this model we used the refractive index $\eta = 2.419$ of diamond [22].

The second reflectance model is controlled by a larger number of parameters, and it is wavelength dependent. It corresponds to an algorithmic model of light propagation in foliar tissues. Its formulation as well as the values assigned to its parameters, which in our experiments correspond to a soybean leaf, are described in a recent paper by Baranoski and Rokne [2]. The wavelength considered in the experiments using this model was $\lambda = 550nm$.

The experiments performed to illustrate the applicability of the proposed bound for the number of sample rays were divided into two sets. In the first set we tested its application in virtual spectrophotometry aimed at the evaluation of reflectance models. As mentioned earlier, this type of application involves the comparison of virtual spectrophotometric measurements with measurements obtained using a real device. This implies that one should assign values for the dimensions of the virtual device as close as possible to the values of the actual device. The values used in our experiments ($r_1 = 8mm$, $r_2 = 12.5mm$ and $D = 100mm$) correspond to values available in the spectrophotometry literature [7, 19, 26].

In the second set of experiments we illustrate the suitability of the proposed bound for applications involving data generation from previously validated reflectance models. For these experiments we simulate collimated rays, *i.e.*, all sample rays used in a given measurement for specified geometrical and spectral conditions have the same origin and hit the specimen at the same point. This type of application usually involves a large number of measurement instances, *e.g.*, measurements for polar angles of incidence, θ_i, varying from 0° to 90° in intervals of 1°. In order to observe the average magnitude of the fluctuations of the resulting curves we use the following formula:

$$\Delta = \frac{\sum_{i=1}^{n} |\rho_i^{(N_j)} - \rho_i^{(N_{j-1})}|}{n} \tag{25}$$

where $\rho_i^{(N_j)}$ and $\rho_i^{(N_{j-1})}$ correspond to reflectance estimates obtained using the ray densities currently and previously applied respectively and n corresponds to the total number of directional-hemispherical reflectance measurement instances.

5. Results and Discussion

Recall that for spectrophotometric measurements aimed at rendering applications an error tolerance of 1% is satisfactory, *i.e.*, $\delta = 0.01$. Also, according to data provided in the spectrophotometry literature [16, 19, 26], the absolute accuracy of actual spectrophotometers is around 0.995, which allows us to set $\mu = 0.005$. Applying the proposed bound (Eq. 24), the number of sample rays required under these conditions is $N = 10^{5.02}$ (or $\log N = 5.02$).

5.1. Measurements of Conical-hemispherical Reflectance

Figures 2-4 present conical-hemispherical reflectance measurements for an incident direction given by $\phi_i = 0^\circ$ and $\theta_i = 70^\circ$, and using different ray densities. As mentioned in Sec. 2.3, in order to increase our scope of evaluations, we applied two different sampling strategies, random and jittering-based, to select the sample points on the disks of the virtual device.

As we can observe in the graphs presented in Fig. 2, we can obtain estimates within the region of asymptotic convergence using the number of rays provided by the proposed bound, *i.e.*, $N = 10^{5.02}$ (or $\log N = 5.02$) On the other hand, we could obtain estimates within the region of constant convergence through the application of a brute-force approach, *e.g.*, using $N = 10^8$ (or $\log N = 8$). The graphs presented in Fig. 3 show, however, that in this case we would have a very significant increase in the processing time required for the virtual spectrophotometric measurements. Therefore, this aspect suggests that we can obtain estimates with a higher reliability/cost ratio using a ray density provided by a bound based on probability theory (Sec. 3).

Moreover, by examining the figures presented in Table 2 for $\delta = 0.01$ and the graphs presented in Fig. 4, we can also verify that the proposed bound, derived from the *exponential* Chebyshev inequality, allows us to obtain estimates with a higher reliability/cost ratio than the bound derived from the ordinary Chebyshev inequality. The practical benefit of using a tighter bound becomes even more noticeable when one works with applications involving a large number of virtual spectrophotometric measurements. In this case, we can obtain highly significant computational savings, in terms of the total processing time, through the use of the ray density provided the proposed bound. Our second set of experiments, which is described next, illustrates this aspect.

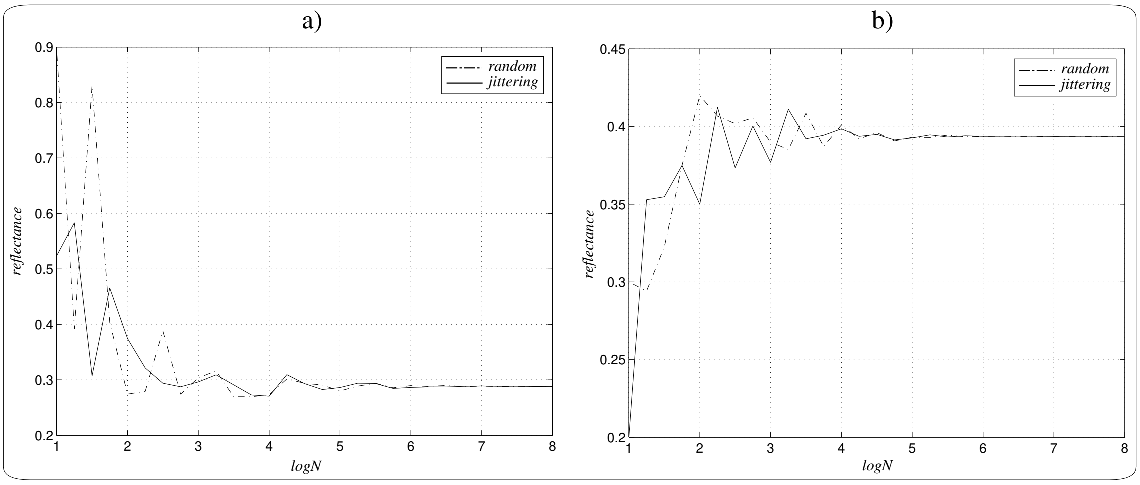

Fig. 2: *Reflectance estimates provided by: a) the simplified reflectance model for dielectrics ($\eta_{diamond} = 2.419$), and b) the algorithmic reflectance model for plant leaves ($\lambda = 550nm$).*

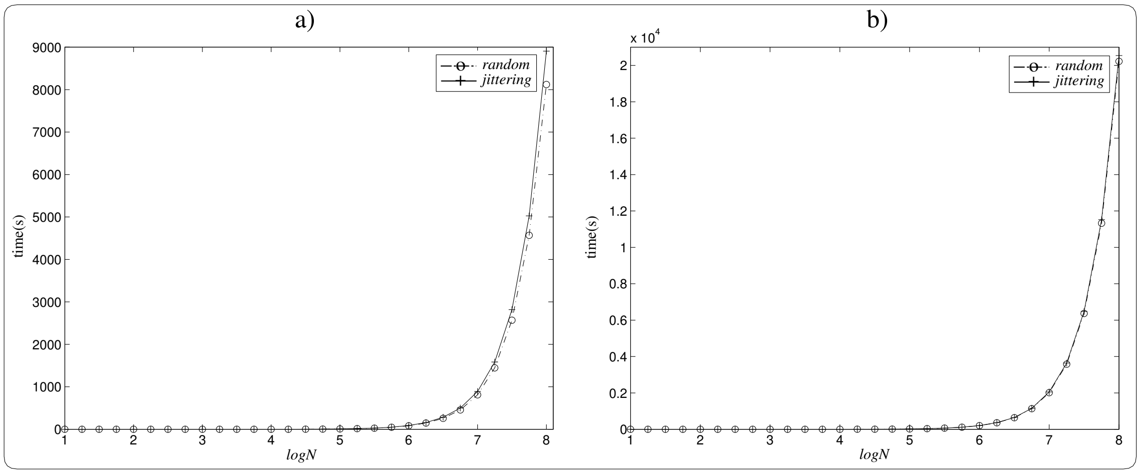

Fig. 3: *Processing times (given by elapsed CPU time on a SGI R5000) associated with the virtual spectrophotometric measurements for: a) the simplified reflectance model for dielectrics, and b) the algorithmic reflectance model for plant leaves.*

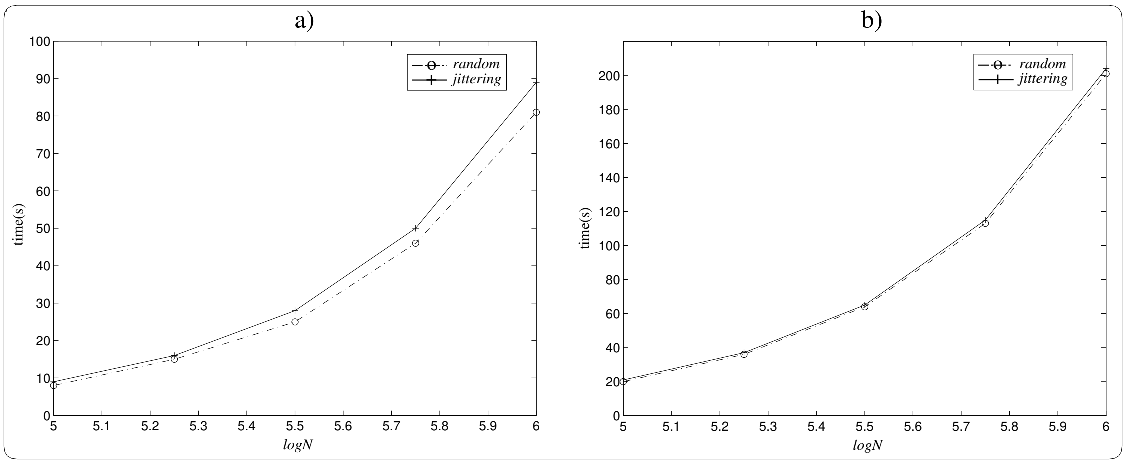

Fig. 4: *Zoom in of the curve of processing times associated with the measurements for: a) the simplified reflectance model for dielectrics, and b) the algorithmic reflectance model for plant leaves.*

5.2. Measurements of Directional-hemispherical Reflectance

Figures 5-6 show the results of directional-hemispherical reflectance measurements when $\phi_i = 0^\circ$ and $\theta_i \in [0^\circ, 90^\circ]$ is sampled at intervals of 1°. For applications involving a large number of measurement instances, such as these, we need to select a ray density that allows minimal fluctuations in the resulting curves. As we can see in Fig. 5, for $N = 10^3$ (or $\log N = 3$) we have very noticeable fluctuations. As we increase the value of N, we start to have smoother curves, and for $N = 10^5$ (or $\log N = 5$) the curves present negligible fluctuations.

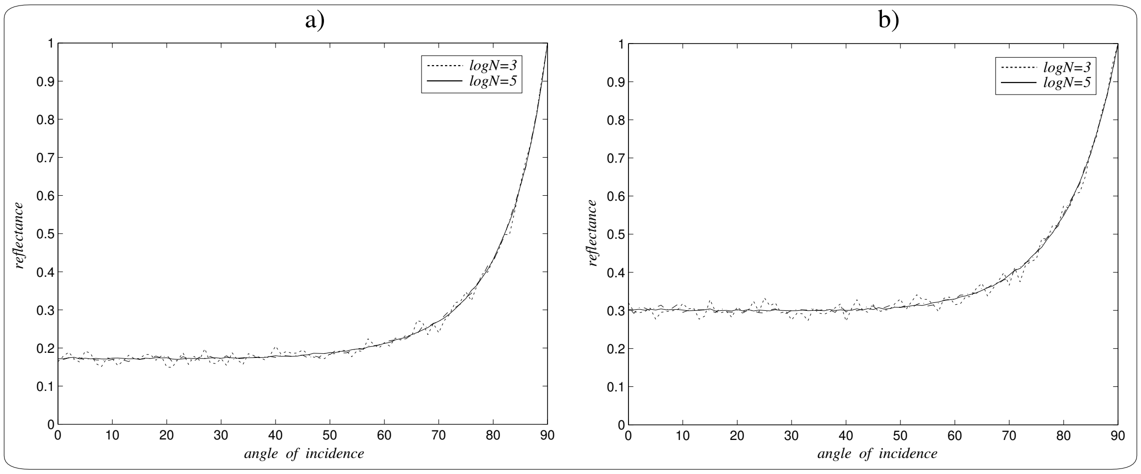

Fig. 5: *Directional-hemispherical reflectance measurements using two different ray densities for: a) the simplified reflectance model for dielectrics ($\eta_{diamond} = 2.419$), and b) the algorithmic reflectance model for plant leaves ($\lambda = 550nm$).*

Increasing the value of N, *e.g.*, using $N = 10^6$ (or $\log N = 6$), we can reduce the fluctuations even more. The graph of the average magnitude of fluctuations, computed using Eq. 25 and presented in Fig. 6a, shows, however, that in this case we would have only a minor reduction in the fluctuations for both reflectance models. Moreover, the graph presented in Fig. 6b shows that in this case we would have a substantial increase in the processing time (around $10\times$) for both reflectance models. These observations suggest that using the ray density given by the proposed bound (Eq. 24) we can obtain results with a reasonably high reliability/cost ratio for this type of applications as well.

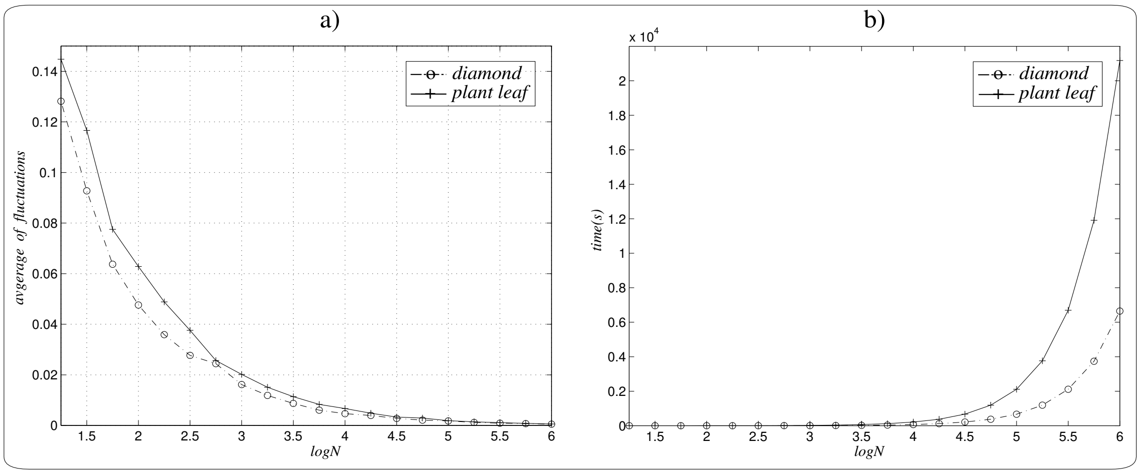

Fig. 6: *a) Average of fluctuations, and b) processing times (given by elapsed CPU time on a SGI R5000) associated with the directional-hemispherical reflectance measurements for the two reflectance models used in our experiments.*

6. Summary and Future Research

A key aspect in rendering is the appropriate consideration of the attributes that determine the appearance of objects and surfaces, such as color. These attributes are directly related to spectral energy distribution of the light reflected and transmitted by an object or surface, which is represented by reflectance and transmittance, respectively, and measured by devices known as spectrophotometers. The correctness of the reflectance and transmittance models is, therefore, a valuable asset in physically-based rendering applications.

In this paper we investigated the computer simulation of spectrophotometers known as virtual spectrophotometers. These devices have a "ray nature" and a formulation based on Monte Carlo methods. Due to their stochastic nature, their reliability and efficiency are directly determined by an appropriate qualitative and quantitative selection of sample rays, which is required to obtain estimates with a desired accuracy under specified spectral and geometrical conditions. Although the application of a brute-force approach to determine the ray density may ensure results within the region of constant convergence, it is highly inefficient. Using tools from probability theory we investigated alternatives to obtain a satisfactory bound for the ray density of virtual spectrophotometers. In other words, this bound should take into account the accuracy and performance requirements of rendering applications. Based on this investigation we proposed a bound, derived from the *exponential* Chebyshev inequality, which provides tighter ray densities than previous probability theory results used in particle transport simulations.

We performed experiments using different sampling strategies and models of reflectance with different levels of complexity to illustrate the applicability of the proposed bound. The conclusions drawn from these experiments suggest that the proposed bound allows us to obtain results with reasonably high reliability/cost ratio. For the cases tested this ratio was significantly higher than the reliability/cost ratios associated with the application of a brute force approach and with the use of a bound based on the ordinary Chebyshev inequality. The experiments also show that the suitability of the proposed bound becomes even more noticeable for applications involving a large number of measurement instances. In many cases the total computation time can be reduced by several orders of magnitude through the application of the proposed bound.

Furthermore, as mentioned above, we used two sampling strategies, random and jittering-based, for selecting the origins and targets of sample rays. Despite the better distribution of sample points provided by the jittering-based strategy [22], our experiments show that, for virtual spectrophotometric applications, both strategies lead to results with a similar rate of convergence. In addition, as one would expect intuitively, our experiments also show that the processing time difference between the two strategies tends to becomes less noticeable as we perform measurements on more complex reflectance models. In these situations most of the processing time is used on the propagation of the sample rays by the models instead of being used on the generation of the rays.

In conclusion, although the main purpose of this paper was to contribute to a better theoretical foundation for fundamental research required for physically-based rendering applications, its results may also be extended to other areas demanding virtual spectrophotometric measurements such as remote sensing and colorimetry. Our future efforts will be focus on the ray density analysis for devices measuring the spatial distribution of light, known as goniophotometers. We also intend to investigate the application of the *exponential* Chebyshev inequality to other rendering problems involving particle transport simulation such as the computation of form factors [3].

References

1. ANSI. Nomenclature and definitions for illuminating engineering. In *ANSI/IES RP-6-1986*. Illuminating Engineering Society of North America, New York, 1986.
2. G.V.G. Baranoski and J.G. Rokne. An algorithmic reflectance and transmittance model for plant tissue. *Computer Graphics Forum (EUROGRAPHICS Proceedings)*, 16(3):141–150, September 1997.
3. G.V.G. Baranoski, J.G. Rokne, and G. Xu. Applying the exponential chebyshev inequality to the nondeterministic computation of form factors. Technical Report 99/638/01, Department of Computer Science, The University of Calgary, Canada, March 1999.
4. L. Carter and E.D. Cashwell. Particle transport simulation with the Monte Carlo method. Technical report, Energy Research and Development Administration, 1975.
5. E.D. Cashwell and C.J. Everett. *A Practical Manual on the Monte Carlo Method for Random Walk Problems*. Pergamont Press, New York, 1959.
6. C.L. Chiang. *An Introduction to Stochastic Processes and Their Applications*. Robert E. Krieger Company, New York, 1980.
7. B.G. Crowther. Computer modeling of integrating spheres. *Applied Optics*, 35(30):5880–5886, 1996.
8. ASTM Standard E284-91C. Standard terminology of appearance. In L.B. Wolff, S.A. Shafer, and G.E. Healey, editors, *Physics-Based Vision Principles and Practice: Radiometry*, pages 146–161, Boston, 1992. Jones and Bartlett Publishers.
9. J. Fendley. An analysis of the measuring procedure for the integrating sphere spectrophotometer. *Solar Energy*, 35(3):281–282, 1985.
10. A.S. Glassner. *Principles of Digital Image Synthesis*. Morgan Kaufmann, San Francisco, 1995.
11. D.G. Goebel. Generalized integrating-sphere theory. *Applied Optics*, 6(1):125–128, January 1967.
12. J.M. Hammerley and D.C. Handscomb. *Monte Carlo Methods*. Wiley, New York, 1964.
13. E Hecht and A. Zajac. *Optics*. Addison-Wesley, Reading, Massachusetts, 1974.
14. B. Hosgood, S. Jacquemoud, G. Andreoli, J. Verdebout, G. Pedrini, and G. Schmuck. Leaf optical properties experiment 93. Technical Report Report EUR 16095 EN, Joint Research Center, European Comission, Institute for Remote Sensing Applications, 1995.
15. R.S. Hunter and R.W. Harold. *The Measurement of Appearance*. John Wiley & Sons, New York, second edition, 1987.
16. D.B. Judd and G. Wyszecki. *Color in Business, Science and Industry*. John Wiley & Sons, New York, third edition, 1975.
17. P. Lalonde and A. Fournier. A wavelet representation of reflectance functions. *IEEE Transaction on Visualization and Computer Graphics*, 3(4):329–336, October 1997.
18. R.S. Longhurst. *Geometrical and Physical Optics*. Longman Group Limited, London, third edition, 1973.
19. D.L. MacAdam. *Color Measurements Theme and Variations*. Springer Verlag, Berlin, 1981.
20. F.E. Nicodemus, J.C. Richmond, J.J. Hsia, I.W. Ginsberg, and T. Limperis. Geometrical considerations and nomenclature for reflectance. In L.B. Wolff, S.A. Shafer, and G.E. Healey, editors, *Physics-Based Vision Principles and Practice: Radiometry*, pages 94–145, Boston, 1992. Jones and Bartlett Publishers.
21. Y. Nievergelt. Radiosity in illuminating engineering. *The UMAP Journal*, 18(2):167–179, 1997.
22. P. Shirley. *Physically based lighting for computer graphics*. PhD thesis, Dept. of Computer Science, University of Illinois, November 1990.
23. P. Shirley. Nonuniform random points via warping. In D. Kirk, editor, *Graphics Gems III*, pages 80–83. Academic Press, 1992.

24. A.N. Shiryaev. *Probability*. Springer-Verlag, New York, second edition, 1996.

25. J.V. Uspensky. *Introduction to Mathematical Probability*. McGraw-Hill, New York, 1937.

26. G.A. Zerlaut and T.E. Anderson. Multiple-integrating sphere spectrophotometer for measuring absolute spectral reflectance and transmittance. *Applied Optics*, 20(21):3797–3804, November 1981.